Carbohydrate Polymers 102 (2014) 762–771

Contents lists available at ScienceDirect

Carbohydrate Polymers

journal homepage: www.elsevier.com/locate/carbpol

# *In situ* synthesis of silver-nanoparticles/bacterial cellulose composites for slow-released antimicrobial wound dressing

Jian Wu[a], Yudong Zheng[a,*], Wenhui Song[b], Jiabin Luan[a], Xiaoxiao Wen[a], Zhigu Wu[c], Xiaohua Chen[d], Qi Wang[a], Shaolin Guo[a]

[a] School of Materials Science and Engineering, University of Science and Technology Beijing, Beijing 100083, PR China
[b] Centre for Nanotechnology & Regenerative Medicine, Division of Surgery & Interventional Science, University College London, London NW3 2QG, UK
[c] Hospital Affiliated to Chinese PLA General Hospital, Beijing 100853, PR China
[d] State Key Laboratory of Advanced Metals and Materials, University of Science and Technology Beijing, Beijing 100083, PR China

ARTICLE INFO

*Article history:*
Received 16 August 2013
Received in revised form 6 October 2013
Accepted 29 October 2013
Available online 6 November 2013

*Keywords:*
Bacterial cellulose
Silver nanoparticles
Antimicrobial activities
Epidermal cells
Biocompatibility

ABSTRACT

Bacterial cellulose has attracted increasing attention as a novel wound dressing material, but it has no antimicrobial activity, which is one of critical skin-barrier functions in wound healing. To overcome such deficiency, we developed a novel method to synthesize and impregnate silver nanoparticles on to bacterial cellulose nanofibres (AgNP-BC). Uniform spherical silver nano-particles (10–30 nm) were generated and self-assembled on the surface of BC nano-fibers, forming a stable and evenly distributed Ag nanoparticles coated BC nanofiber. Such hybrid nanostructure prevented Ag nanoparticles from dropping off BC network and thus minimized the toxicity of nanoparticles. Regardless the slow $Ag^+$ release, AgNP-BC still exhibited significant antibacterial activities with more than 99% reductions in *Escherichia coli*, *Staphylococcus aureus* and *Pseudomonas aeruginosa*. Moreover, AgNP-BC allowed attachment and growth of epidermal cells with no cytotoxicity emerged. The results demonstrated that AgNP-BC could reduce inflammation and promote wound healing.



## 1. Introduction

Bacterial cellulose (BC), a natural biopolymer synthesized in abundance by different strains of bacteria's namely *Acetobacter strains* (Brown, 1886), displays high water content (98–99%), good sorption of liquids, high wet strength, high chemical purity and can be safely sterilized without any change of its structure and properties. Due to these special properties, a wide variety of applications have been proposed from paper and textiles (Cheng, Catchmark, & Demirci, 2011; Jung, Kim, Kim, Kwon, Lee, & Jin, 2008), diaphragms for electroacoustic transducers (Ciechanska et al., 2002), coatings (Hu, Chen, Liu, Ding, & Wang, 2011), cosmetics (Boonme, Amnuaikit, Chusuit, & Raknam, 2011), optically transparent composites (Retegi et al., 2012), to e-paper (Shah & Brown, 2005), etc. Recently, there is also an increasing research interest in developing a wide range of biomedical applications, such as tissue-engineering scaffolds (Andersson, Stenhamre, Backdahl, & Gatenholm, 2010; Bodin, Bharadwaj, Wu, Gatenholm, Atala, & Zhang, 2010; Brackmann, Zaborowska, Sundberg, Gatenholm, & Enejder, 2012; Shi et al., 2012; Zaborowska, Bodin, Backdahl, Popp, Goldstein, & Gatenholm, 2010), artificial blood vessels (Klemm, Schumann, Udhardt, & Marsch, 2001) and wound dressings for wounds (Solway, 2010) and burns (Muangman, Opasanon, Suwanchot, & Thangthed, 2011).

In the processing of skin tissue repair, the moisture environment provided by the dressing has been shown to promote ulcers healing and reduce pain of patients (Czaja, Krystynowicz, Bielecki, & Brown, 2006). The intrinsic properties of BC mentioned above make it an attractive novel wound-dressing material. However, lack of antimicrobial activity of BC is the main issue to be tackled, which is critical to provide a bacteria-proof barrier to the outside world in wound-healing (Robson, 1997). In burns patients with extensive skin loss, bacterial sepsis can be fatal. To solve this problem, researches have introduced different materials such as benzalkonium chloride (Wei, Yang, & Hong, 2011), chitosan (Cai, Hou, & Yang, 2012) and metallic nanoparticles into BC. Among them, metallic nanoparticles such as copper-, silver and ZnO have been recently reported as excellent antimicrobial agents (Ghule, Ghule, Chen, & Ling, 2006; Ruparelia, Chatterjee, Duttagupta, & Mukherji, 2008; Zhang, Peng, Huang, Zhou, & Yan, 2008), owing to their nanoscale structure and large surface area to volume ratio comparing to their bulk form. In particular, silver nanoparticles (AgNPs) have been intensively studied due

* Corresponding author. Tel.: +86 10 62330802.
*E-mail addresses:* wujian.ustb@gmail.com (J. Wu), zhengyudong@mater.ustb.edu.cn (Y. Zheng), wh_song@hotmail.com (W. Song), luanjiabin@gmail.com (J. Luan), yujilingyujiuyou@126.com (X. Wen), wzhigu@yahoo.com.cn (Z. Wu), chenxh@skl.ustb.edu.cn (X. Chen), 15201461928@163.com (Q. Wang), ustbgsl@163.com (S. Guo).

0144-8617/$ – see front matter © 2013 Elsevier Ltd. All rights reserved.
http://dx.doi.org/10.1016/j.carbpol.2013.10.093

to its strong antimicrobial activities toward many different bacteria, fungi, viruses, and several antibiotic resistant strains (Damm, Munsted, & Rosch, 2007; Klasen, 2000; Kumar, Vemula, Ajayan, & John, 2008; Panyala, Pena-Mendez, & Havel, 2008). However, the aggregation tendency of AgNPs can undermine their unique properties at nanoscale. One strategy to prevent aggregation is the controlled deposition of metal particles through hybridization by using a nanoporous material as template to ensure a well-defined spatial distribution (Cai, Kimura, Wada, & Kuga, 2009). Sheet-shaped BC supports can make it easy to incorporate nano-sized metallic particles (Ifuku, Tsuji, Morimoto, Saimoto, & Yano, 2009). Researchers have proposed several methods to obtain the AgNPs impregnated BC composites through $NaBH_4$ and UV radiation (Pinto, Marques, Neto, Trindade, Daina, & Sadocco, 2009); triethanolamine (TEA) (Barud, Regiani, Marques, Lustri, Messaddeq, & Ribeiro, 2011); self-polymerized polydopamine (Sureshkumar, Siswanto, & Lee, 2010); hydrazine, hydroxylamine or ascorbic acid (de Santa Maria, Santos, Oliveira, Barud, Messaddeq, & Ribeiro, 2009); TEMPO-mediated oxidized BC followed by thermal reduction (Ifuku et al., 2009).

For impregnation, most of these studies utilized the electrostatic interactions between metallic ions and dipole moments of cellulose molecules and the nanospace in the cellulose fibers served as nanoreactor (Jung, Kim, Kim, & Jin, 2009; Maneerung, Tokura, & Rujiravanit, 2008; Pinto et al., 2009; Sureshkumar et al., 2010; Yang, Xie, Hong, Cao, & Yang, 2012). However, the anchor metallic ions on cellulose fibers generated through these methods are normally weak (de Santa Maria et al., 2009), resulting in a low yield and sparse distribution of metallic nanoparticles (Ifuku et al., 2009). Besides, it has been reported that silver is a recognized cause of argyrosis and argyria (Cohen, Quentel, Egasse, Cadot, Ingster-moati, & Coscas, 1993; Rosenman, Moss, & Kon, 1979) and a high concentration of silver nanoparticles is toxic to mammalian cells (Ahamed et al., 2008). Thus, the weak interaction between AgNPs and BC may cause cell toxicity due to the instability and uncontrollable release of AgNPs, which has not been tackled up to now.

In this work, we put forward a new method of producing silver nanoparticle/bacterial cellulose (AgNP-BC) hybrid gel-membrane, aiming to improve the antimicrobial activity of bacterial cellulose, while to avoid the over-quick release of $Ag^+$ and therefore to reduce the toxicity of nanoparticles. Silver nanoparticles were synthesized *in situ* through the reaction of Tollens' reagent with bacterial cellulose acting as nano-reactive template. Such reaction formed a stable and strong interaction between uniformly distributed spherical silver nano-particles and BC fibers, in the evidence of well-controlled $Ag^+$ release, no cell toxicity of nanoparticles and growth of epidermal cells. The synthesis process and structure of AgNP-BC were investigated by XRD, SEM, FT-IR as well as EDS tests. *In vitro* Ag releasing properties of AgNP-BC and control samples were measured in PBS buffer solution. The antibacterial activities of AgNP-BC against *Escherichia coli*, *Staphylococcus aureus* and *Pseudomonas aeruginosa* were demonstrated by disk diffusion and shake flask test method. Effects of AgNP-BC on cell growth were investigated through cultivation of epidermal cells.

## 2. Materials and methods

### 2.1. Materials

Bacterial cellulose was offered by Hainan Yida Food Co. Ltd. (China). Silver nitrate ($AgNO_3$) and sodium hydroxide (NaOH) were purchased from Sinopharm Chemical Reagent Beijing Co. Ltd. Diamine Tetraacetic Acid (EDTA), Ethylene Tetrazolium Bromide (3-(4,5-dimethyl-2-thiazolyl)-2,5-diphenyl-2H, MTT), and trypsin were offered by Merck. Dulbecco's modified eagle medium (DMEM) was purchased from Gibcobrl. All other reagents and solvents were purchased from the domestic suppliers and used as received.

**Table 1**
Content of Ag in different samples.

| Code | Sample | Ag (Wt.%) | Ag content (mg/100 cm$^2$) |
|---|---|---|---|
| $C_0$ | BC | – | – |
| $C_1$ | $AgNO_3$-BC | 1.09 | 14.85 ± 1.93 |
| $C_2$ | nAg-BC | 1.12 | 15.31 ± 2.16 |
| $S_1$ | AgNP-$BC_{0.01}$[a] | 1.01 | 18.72 ± 1.36 |
| $S_3$ | AgNP-$BC_{0.03}$[a] | 2.62 | 30.76 ± 1.47 |
| $S_5$ | AgNP-$BC_{0.05}$[a] | 3.40 | 45.27 ± 2.01 |

[a] AgNP-$BC_x$, the subscript $x$ indicates the concentration of Tollens' reagent.

### 2.2. In situ formation of silver nanoparticles into BC

The bacterial cellulose membranes were washed with deionized water and then immersed in 0.1 N NaOH solution at 100 °C for 1 h to remove the impurities such as medium, endotoxin et al. on the membranes. Finally, samples were rinsed with deionized water to pH = 7 and stored in deionized water at room temperature prior to further experimentation. Silver ammonia solution (Tollens' reagent, 0.1 mol/L) was prepared and then diluted to 0.01 mol/L, 0.03 mol/L and 0.05 mol/L respectively before usage. The purified BC membranes were soaked in silver ammonia solution of different concentrations for 24 h and then thoroughly washed to remove residual chemicals on surface. Subsequently, BC membranes were kept in a warm water bath at 80 °C for 10 min, and after then the resulting membranes were washed with running deionized water to remove the residual chemicals. AgNP-BC hybrid gel-membranes were obtained (Table 1: $S_1$, $S_3$, $S_5$). Samples with defined dimensions were dissolved by 1 mL concentrated sulfuric acid. Contains of Ag in the acquired solution were determined by flame atomic absorption spectrophotometry (AA300, Perkin Elmer, USA). The results obtained were listed in Table 1.

### 2.3. Structure of AgNP-BC

The structure of AgNP-BC was studied by a Rigaku D/max-RB X-ray diffractometer (Rigaku Corporation, Japan). The samples were scanned from 10° to 70° at the speed of 10°/min. The data were processed using MDI/JADE6.0 software package. FT-IR spectra of samples prepared by KBr method were measured with SPECTRUM ONE (USA) infrared spectrometer between 4000 and 450 $cm^{-1}$ at a resolution of 4 $cm^{-1}$. Samples were dehydrated by solvent exchange (70% ethanol → 100%) and then kept in Electric Thermostatic Drier at 20 °C. For improved contrast, the gold was sputtered on samples before analysis. SEM pictures were taken at different magnifications with an Apollo 300 scanning electron microscope (UK). Elemental maps of the silver nanoparticles in BC were obtained using energy dispersive spectrometer (EDS, Oxford).

### 2.4. Release of silver in vitro

For investigation of the silver release of AgNP-BC *in vitro*, two kinds of BC composite membranes were prepared as control groups to compare with AgNP-BC (Table 1: $C_1$, $C_2$). $C_1$ (control group No. 1, $AgNO_3$-BC): BC membranes were immersed in $AgNO_3$ aqueous solution (0.1 mol/L) for 1 h and then excess liquid was removed from the surface by filter paper to attain BC membrane containing $AgNO_3$. $C_2$ (control group No. 2, nAg-BC): BC membranes were immersed in Ag nanoparticle aqueous suspensions (Ag nanoparticle was obtained from Shanghai Huzheng Nanotechnology Co., Ltd. 1000 ppm, 10–20 nm) for 1 h. Then the membrane was taken out, removed the excess liquid on the surface by filter paper to produce BC membrane containing Ag nanoparticles. (nAg-BC).

The kinetics of silver release was studied from the prepared BC samples. AgNP-$BC_{(0.01)}$, AgNP-$BC_{(0.03)}$, AgNP-$BC_{(0.05)}$, $AgNO_3$-BC, nAg-BC membranes were cut into round pieces in diameter of 10 mm. These samples were then immersed in 10 mL phosphate buffered saline (PBS, pH = 6.0) at 37 °C. 0.2 mL solution was taken at regular time intervals (0.5, 1, 2, 3, 6, 12, 24, 48 and 72 h) and analyzed for the amount of Ag released using flame atomic absorption spectrophotometry (FAAS), and then the same volume of fresh phosphate buffered saline solution was added.

Another silver release test was conducted in circulated PBS medium. PBS medium was completely replaced with fresh PBS periodically at each sampling time (every 12 h) for 10 times in order to test the persistence of silver releasing property of the samples. The amount of Ag released was analyzed every 12 h before PBS circulation using flame atomic absorption spectrophotometry (FAAS).

### 2.5. Antimicrobial activity studies

The antimicrobial activity of the composite membranes was investigated against *E. coli*, *S. aureus* and *P. aeruginosa*, using two methods. In the disk diffusion method (ISO 20645:2004), and a commercial silver-containing dressing (Coloplast® Ag non-adhesive foam dressing) was setted as a positive control. The test specimen and pure BC (control samples) were cut into a disk shape with 6.5 mm diameter, sterilized by autoclaving for 20 min at 121 °C. Before culturing in an incubator at 37 °C for 24 h, samples were pressed into intimate contact with an agar culture medium inoculated with the *E. coli*, *S. aureus* and *P. aeruginosa* solution. Subsequently, the zone of bacterial inhibition was monitored.

In the shake flask test method (ASTM E2149-01), 2.5 mL of the bacteria inoculum was added to a test flask containing 0.4 g test specimen. After sampling at time zero, the numbers of the bacteria were counted by placing and incubating on an agar plate. The same procedure was repeated for the control samples. Then, all the flasks were shaken for 24 h and the numbers of living bacteria were counted. The reduction percentage in bacterial count and bacteriostatic rate were determined using the following formula:

$$\text{Reduction of bacteria} = \frac{B - A}{B} \times 100\%$$

$$\text{Bacteriostatic rate} = \frac{C - A}{C} \times 100\%$$

where: *A*, colony forming unit counts/mL (CFU/mL) of the samples at 24 h; *B*, CFU/mL of the samples at 0 h; *C*, CFU/mL of $C_0$ at 24 h.

### 2.6. Cultivation of epidermal cells

Cultivation of epidermal cells was designed to investigate possible effects of the samples on epidermal growth. Three-days-old newborn Westar fetal rats (Experimental Animal Center of Military Medical Sciences, China; no special gender requirement) were sacrificed by Cervical dislocation, and then soaked in 75% ethanol for 3 min. Following experiments were all done under aseptic conditions. After rinsing with saline water, the entire skins were cut off from the body with hypodermis scraped off and chopped into pieces (0.5 cm × 2 cm). The pieces were immersed in blended solution of 0.25% trypsin and 0.02% EDTA and then stored in the fridge at 4 °C for 16 h. After that, epidermis, separated from the pieces of skin, was put in a container with DMEM. After counting under the inverted microscope, epidermis suspension was centrifuged for 5 min at the speed of 1000 r/min. DMEM, containing 10% fetal calf serum, was added to dilute the cell density to $1 \times 10^5$/mL.

Epidermal cell suspension (1 mL) was inoculated in a 24-well plate. After precipitation for 1 h in epidermal cells suspension, different samples were put in corresponding plates and cultured in 5% $CO_2$ incubator at 37 °C for 1, 4, 7 and 10 days, respectively. The culture medium was changed on the 4th and 7th day.

To observe cell morphology and distribution, epidermal cells cultured for 1, 4, 7 and 10 days were observed respectively by using a Leica DMI 4000 semi-automatic inverted biological microscope (Germany). Culture medium was replaced with 0.5 mL blended solution of 0.25% trypsin and 0.02% EDTA. 10 min later, 0.5 mL fetal calf serum-DMEM was added to terminate the digestion. The number of cells was counted using blood counting chamber direct counting method ($10^5$ cells/well).

Cell viability was tested by MTT assays on 1, 4, 7 and 10 days, respectively. Briefly, 100 μL of MTT (3-(4,5-dimethyl-2-thiazolyl)-2,5-diphenyl-2H tetrazolium bromide, 5 mg/mL) was added into each well followed by 4 h incubation at 37 °C in 5% $CO_2$ incubator. Subsequently, the medium was removed carefully and 500 μL of DMSO (dimethyl sulfoxide) was added to dissolve the formazan formed previously. Solubilized formazan products were quantified by spectrophotometry at 570 nm using an ELx800 Universal Microplate Reader (Bio-TEK instruments, INC., USA). Cells cultured with medium alone were used as control and the cell viability was considered as 100%.

### 2.7. Statistical analyses

Statistical analysis of data was performed by one-way analysis of variance (ANOVA), assuming confidence level of 95% ($p < 0.05$) for statistical significance. All the data were expressed as means ± standard deviation (SD).

## 3. Results and discussion

### 3.1. Synthesis and structure of AgNP-BC

Fig. 1(A–C) illustrates the chemical reactions involved in the formation of silver nanoparticles in BC. It is envisaged that guest molecules of Tollens' reagent diffused into the inner spaces of BC nanopores and reacted with cellulose fibers (Fig. 1(A)), and BC played a role of reactive template at nanoscale during the formation of silver nanoparticles (Fig. 1(B) and (C)). Purified BC membranes were initially soaked in Tollens' reagent for 24 h resulting in the attachment of $Ag(NH_3)_2^+$ to BC fibers by a chemical bond (Fig. 1A). In this process, $Ag(NH_3)_2OH$, as a weak oxidant, was likely to react with the hydroxyl in $C_6$ of BC (Fig. 1(B), (1)), and $-CH_2-OH$ was firstly oxidized to aldehyde group ($-CH=O$), which could further react with $Ag(NH_3)_2OH$ (Fig. 1(2)). In the meantime, metallic silver were generated in the nanopores, and tended to adhere to the surface of BC fibers, forming silver seeds (showed in Fig. 1(B)). Subsequently, BC membranes was kept in a warm water bath at 80 °C for 10 min. BC could continue to react with $Ag(NH_3)_2OH$ to form more Ag. Silver nanoparticles (AgNPs) were gradually generated and closely deposited on BC nano-fibers, forming a stable and uniform Ag nanoparticles/BC hybrid as illustrated in Fig. 1(C) and proven by the following observation by scanning electron microscopy (Fig. 2).

Fig. 2(A)–(D) shows SEM micrographs of morphology of BC and AgNP-BC. BC nanofibres form interconnective porous structure with pore size in a range of 100s nanometers, as shown in Fig. 2(A). Such 3D network allowed guest molecules to diffuse throughout its inner space easily. After BC membranes being soaked in $Ag(NH_3)_2OH$ for 24 h, silver seeds and nanoparticles emerged to adhere to the surface of BC fibers (Fig. 2(B)), indicating strong affinity between Ag and BC fibers. The following warm water bath procedure accelerated the reactions and deposition of silver nano-particles (AgNPs) on the nanofibres. As shown in Fig. 2(C),

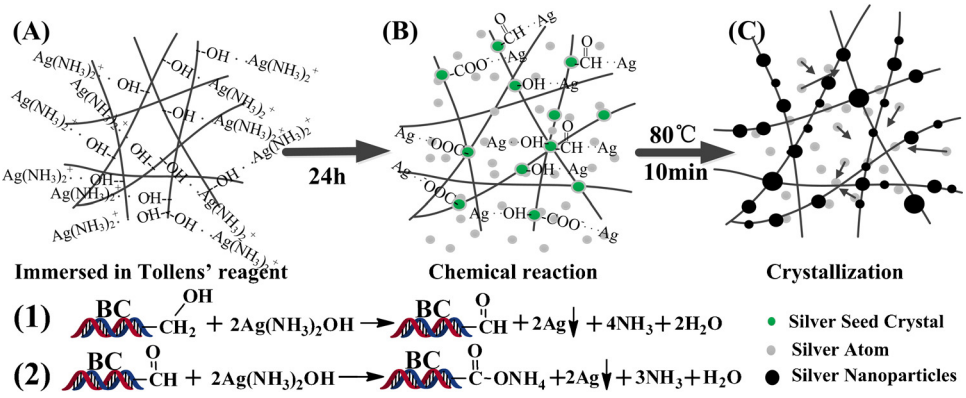


**Fig. 1.** Synthetic procedure and chemical equations of silver nanoparticles generated in AgNP-BC.

the hybrid nanostructure of resulting AgNP-BC consisted of stable, uniform spherical silver nano-particles evenly distributed and anchored on BC nano-fiber 3D network. The granularity analysis (by image-pro plus 6.0) results showed that the particle diameter of more than 75% silver nano-particles generated in BC nano-fibers was in the range of 10–30 nm (the inset image in Fig. 2(C)). EDS-analysis of AgNP-BC further confirmed the existence of silver in BC membranes (the inset image in Fig. 2(D)).

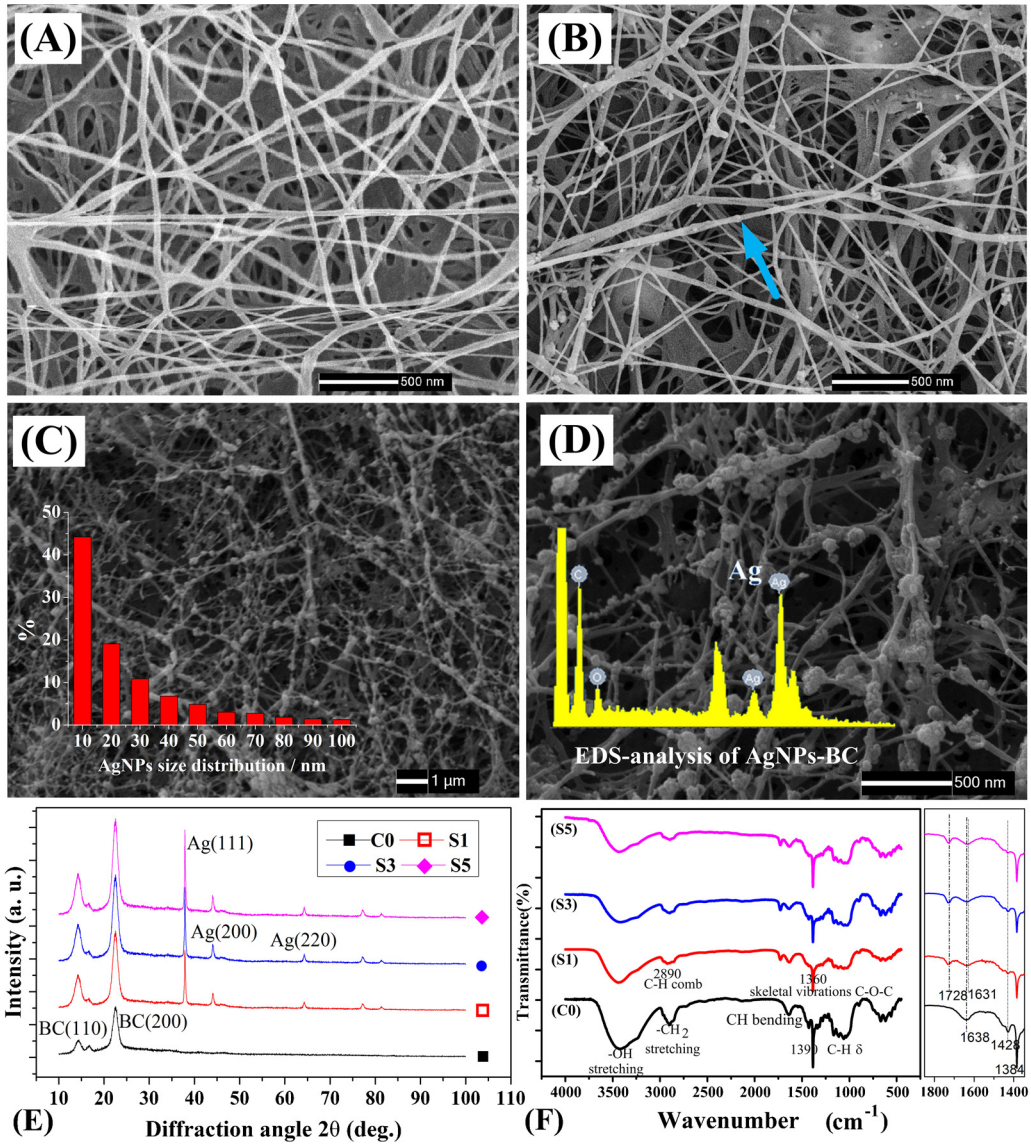


**Fig. 2.** Scanning electron microscopic morphology of (A) bacterial cellulose; (B) BC membranes soaked in Tollens' reagent; (C) AgNP-$BC_{(0.03)}$ (20000X); (D) AgNP-$BC_{(0.03)}$ (50000X) and EDS-analysis of AgNP-BC; (E) XRD patterns of bacterial cellulose and AgNP-BC composite materials, (F) FT-IR spectra of bacterial cellulose and AgNP-BC composite materials. ($C_0$: BC; $S_1$: AgNP-$BC_{(0.01)}$; $S_3$: AgNP-$BC_{(0.03)}$; $S_1$: AgNP-$BC_{(0.05)}$).

X-ray diffractogram of dry BC membranes showed three characteristic peaks (Fig. 2(E)) locating at 14.60°, 16.82° and 22.78° corresponding to (1 1 0), (1 $\bar{1}$ 0) and (2 0 0) crystal planes of cellulose (Fig. 2(E) – $C_0$). This is consistent with the experimental results reported by many literatures (Ul-Islam, Ha, Khan, & Park, 2013; Yan, Chen, Wang, Wang, & Jiang, 2008; Yang, Jia, Xing, Chen, & Lu, 2013; Yoshino et al., 1990). According to Bragg's law, identity distance of each crystal plane is 0.606 nm, 0.527 nm and 0.390 nm, demonstrating the existence of a typical cellulose I crystal (Isogai, Usuda, Kato, Uryu, & Atalla, 1989; Shezad, Khan, Khan, & Park, 2010). The degree of crystallinity of BC membranes calculated by jade6.0 software is 85.77%. X-ray diffractogram of AgNP-BC also shows the same characteristic peaks of cellulose I crystal. Crystallinity of BC in AgNP-BC is 83.68–86.21%, and thus there is no obvious difference in crystallinity of pure BC and AgNP-BC membranes. It is clear that the crystal structure and crystallinity degree of BC has not been interfered during the in *situ* synthesis of Ag, which is highly desirable in order to preserve those outstanding properties of BC. Five more sharper characteristic peaks could be seen in Fig. 2(E) – $S_1$, $S_3$, $S_5$, at wider Bragg angles of 38.1°, 44.2°, 64.2°, 77.5°, 81.5°, which respectively corresponded to (1 1 1), (2 0 0), (2 2 0), (3 1 1) and (2 2 2) crystal planes on the basis of face–centered cubic (fcc) structure of silver. These results further proved that metallic crystalline silver was produced in BC network.

Fig. 2(F) shows the FT-IR spectra of bacterial cellulose and its AgNP-BC composite materials. The detail analysis of those spectra evidenced that the hydroxyl groups at $C_6$ of cellulose could be converted to carboxylate groups through the redox reaction. The weak characteristic peaks at 1720–1760 $cm^{-1}$ in FT-IR spectra of AgNP-BC hybrid materials (Fig. 2(F) – $S_1$, $S_3$, $S_5$) indicated the existence of carboxylate groups due to the C=O stretching vibration. In contrast, no absorption peaks are observed at 1720–1760 $cm^{-1}$ in purified BC (Fig. 2(F) – $C_0$). Those new absorption peaks imply the oxidation of BC which supports the reaction of $Ag(NH_3)_2OH$ with hydroxyl in $C_6$ of BC (Fig. 1(1)). Meanwhile, the intensity of band near 1320–1210 $cm^{-1}$ associated with the bond stretching of the C—O group decreased obviously. The absorption peaks at 3459, 1660, and 2890 $cm^{-1}$ (Fig. 2(F) – $S_1$, $S_3$, $S_5$) corresponding to stretching-shrinking vibrations of —OH groups and hydrogen bond also decreased in AgNP-BC, which was attributed to the decrease of —OH of cellulose chains involved in the reaction with $Ag(NH_3)_2OH$. Furthermore, the absorption peaks at 1426, 1362, and 1317 $cm^{-1}$ were assigned to symmetric bending and wagging vibrations of $—CH_2—$ groups in the $C_6$ of BC chains. A reduction of vibrations of $—CH_2—$ groups after the reaction suggested that the reaction occurred in the $C_6$ of BC chains, which further proved the reaction of Fig. 1(1) and (2).

A number of nanomaterials are reported to be potentially harmful due to their influence on organisms in levels of cell, subcellular fraction and protein (Maynard et al., 2006). The cell toxicity is of crucial concern due to the high surface area to volume ratio of the nanomaterials (Wijnhoven et al., 2009). The strong adhesion between Ag and BC nanofibers observed above holds a promise to prevent Ag nanoparticles leaching from BC network and entering organisms, which is imperative for the application of AgNP-BC in biomedical field. The subsequent results of Ag releasing and cytotoxicity tests support our hypothesis.

### 3.2. *In vitro* Ag releasing properties of AgNP-BC

In order to investigate Ag release behavior of AgNP-BC, two kinds of silver-containing BC membranes through direct diffusion/absorption methods were prepared as control groups, which were BC membrane containing $AgNO_3$ ($AgNO_3$-BC) and BC membrane containing Ag nanoparticles (nAg-BC) (as described in Section 2.2). Fig. 3(A)–(C) shows SEM micrographs of the three types of silver-containing BC membranes. As discussed above, *in situ* reaction and deposition method produced the hybrid nanostructure with uniform spherical silver nanoparticles evenly adhered on to BC nano-fibers in AgNP-BC (Fig. 3(A), AgNP-$BC_{(0.03)}$). BC membrane was immersed in Ag nanoparticle suspension (nAg-BC), and Ag nanoparticles adsorb to the surface of BC nano-fibers through electrostatic adsorption (Fig. 3(B)); and for $AgNO_3$-BC, $AgNO_3$ diffused into BC fiber network, crystallized and covered the almost whole area of dehydrated BC gel-membrane (Fig. 3(C)).

$Ag^+$ releasing profiles of different samples in PBS solution were presented in Fig. 3(D) and (E), the release of samples followed an exponentially increase with the release time, which depended on Ag loading method and content, *i.e.* released $Ag^+(t) \propto t^n$, after some hours, the release is near to linear. The power law exponent, $n$, the slope of a linear fitting between log ($Ag^+$) and log $t$, and fitting coefficient $R^2$ calculated and listed in Table 2. The results show that $n$ varied for different samples which is indicative of different transport mechanism. The power law exponent for $Ag^+$ release of AgNP-BCs is between 0.638 and 0.802, with $R^2$ of fitting coefficient >0.99%, indicating the high static correlation between the exponential power law and experimental measurements. Such release power laws do not closely follow $t^{1/2}$ time dependence of physical diffusion-controlled drug transport of a polymer thin film based on the Higuchi equation or pure Fick's second diffusion law in a thin polymer film (Paul, 2011; Siepmann & Peppas, 2011). The power law of $Ag^+$ releasing rate of nAg-BC is 0.460 with $R^2 = 0.986$, which seems closer to $t^{1/2}$ time dependence diffusion-controlled model. Anormalous transport of the power law of $Ag^+$ releasing rate of $AgNO_3$-BC was obtained with $n = 0.134$ and a low fitting coefficient ($R^2 = 0.866$), which may be attributed to predominant and rapid dissolution of a large excess of free $AgNO_3$ absorbed on the surface of the membrane at the early stage of release. The $Ag^+$ releasing amount of $AgNO_3$-BC started to level off and reached a plateau after about 2 h, in contrast to 72 h for AgNP-BC and nAg-BC. The $Ag^+$ release of AgNP-BC in PBS solution was slowed down significantly with a gradual increase of release concentration of $Ag^+$ over time, which means $Ag^+$ was released in a controllable way. Table 2 shows the release ratio of $Ag^+$ from BC, in which 15.1–18.6% of $Ag^+$ was released from AgNP-BC in 72 h, but 65.2% and 81.8% from nAg-BC to $AgNO_3$-BC respectively for the same period of time. The correlation between the exponent, $n$, of release power law of AgNP-BC with different Ag content is also established as show in Table 2. From samples $S_1$, $S_3$ and $S_5$ in Tables 1 and 2, the higher Ag content of AgNP-BC, the relatively faster $Ag^+$ release.

Fig. 3(F) shows distinctly different silver releasing profiles of AgNP-BC and control samples in the circulated PBS buffer solution, and reflects the sustained release properties of silver ions from AgNP-BC. From Fig. 3(F), AgNP-BC ($S_1$, $S_3$, $S_5$) retained a high and stable $Ag^+$ releasing quantity even after PBS circulation for several times. Average quantities of $Ag^+$ release from $S_1$, $S_3$, $S_5$ were about 10, 15, 20 μg every time respectively. The results reveal the outstanding sustained release properties of $Ag^+$ from AgNP-BC. For $C_1$ and $C_2$ samples, the release quantities of $Ag^+$ dropped drastically after circulation for three times and then reached a stable level with little silver ion released. About 58.1–69.2% of silver was released from AgNP-BC after circulation for ten times, in contrast to 82.9% and 99.1% of $Ag^+$ released from nAg-BC to $AgNO_3$-BC respectively.

Generally, the silver content was tested by flame atomic absorption spectrophotometry (FAAS), but nonionic Ag particles could not be tested by FAAS. To test the content of nonionic Ag particles, nitric acid was applied to ionize particles before testing. The difference of silver content before and after reacted with nitric acid shows the existence of nonionic silver in the solution which should be the free Ag particles leached from BC fibers because of their weak interaction. The differences of $Ag^+$ release quantity from three

**Table 2**
Release quantity and release ratio of Ag from AgNP-BC and control groups after 3 day and 10 times; slope of fitting and fitting coefficient of log (release quantity of $Ag^+$) *vs* log (times) curve. ($C_1$: $AgNO_3$-BC; $C_2$: nAg-BC; $S_1$: $S_3$: AgNP-$BC_{(0.03)}$; $S_1$: AgNP-$BC_{(0.05)}$).

| Samples | Silver content (μg) | 3 day | | | | After 10 times | |
|---|---|---|---|---|---|---|---|
| | | Release quantity (μg) | Release ratio (%) | Slope of fitting ($n$) | Fitting coefficient ($R^2$) | Release quantity (μg) | Release ratio (%) |
| $C_1$ | 116.57 | 95.39 | 81.8 | 0.134 | 0.866 | 115.47 | 99.1 |
| $C_2$ | 120.18 | 78.35 | 65.2 | 0.460 | 0.986 | 99.58 | 82.9 |
| $S_1$ | 146.95 | 27.34 | 18.6 | 0.638 | 0.991 | 101.73 | 69.2 |
| $S_3$ | 257.17 | 38.86 | 15.1 | 0.703 | 0.996 | 152.63 | 59.3 |
| $S_5$ | 355.37 | 54.79 | 15.4 | 0.802 | 0.997 | 206.64 | 58.1 |

kinds of samples in PBS buffer solution were tested before and after treatment with nitric acid after 72 h, as shown in Fig. 3(G). For nAg-BC, the release amount of $Ag^+$ after dissolved with nitric acid is greater than that before any treatment, which implied that some loosely-attached Ag nanoparticles diffused into PBS solution from nAg-BC. However, $Ag^+$ concentration in PBS solution released from AgNP-BC was almost the same before and after nitric acid treatment, indicating that very little free Ag nanoparticles entered PBS solution directly. These were further supported by the results of laser particle size distributing test of the releasing solution at 72 h (Fig. 3(H)). The results show that there were few particles in the releasing solution of AgNP-BC, in contrast, a large number of particles were detected in the releasing solution of nAg-BC. This provides sheer evidence of strong adhesion between Ag nanoparticles and BC nano-fiber generated through *in situ* formation and self-assembly of Ag based on reactive BC nanofibre template. Such strong adhesion prevented leakage of Ag nanoparticles from the membrane, which can potentially avoid an issue of biotoxicity of nanomaterials, a current major concern for real world applications of nanomaterials (Hussain et al., 2009). This also proved that the release formulation of AgNP-BC was Ag nanoparticle ionization chemical process. There is bound to have discrepancies compared with Fickian physical diffusion model as $Ag^+$ release is predominantly chemically controlled. For nAg-BC, the ionization took place

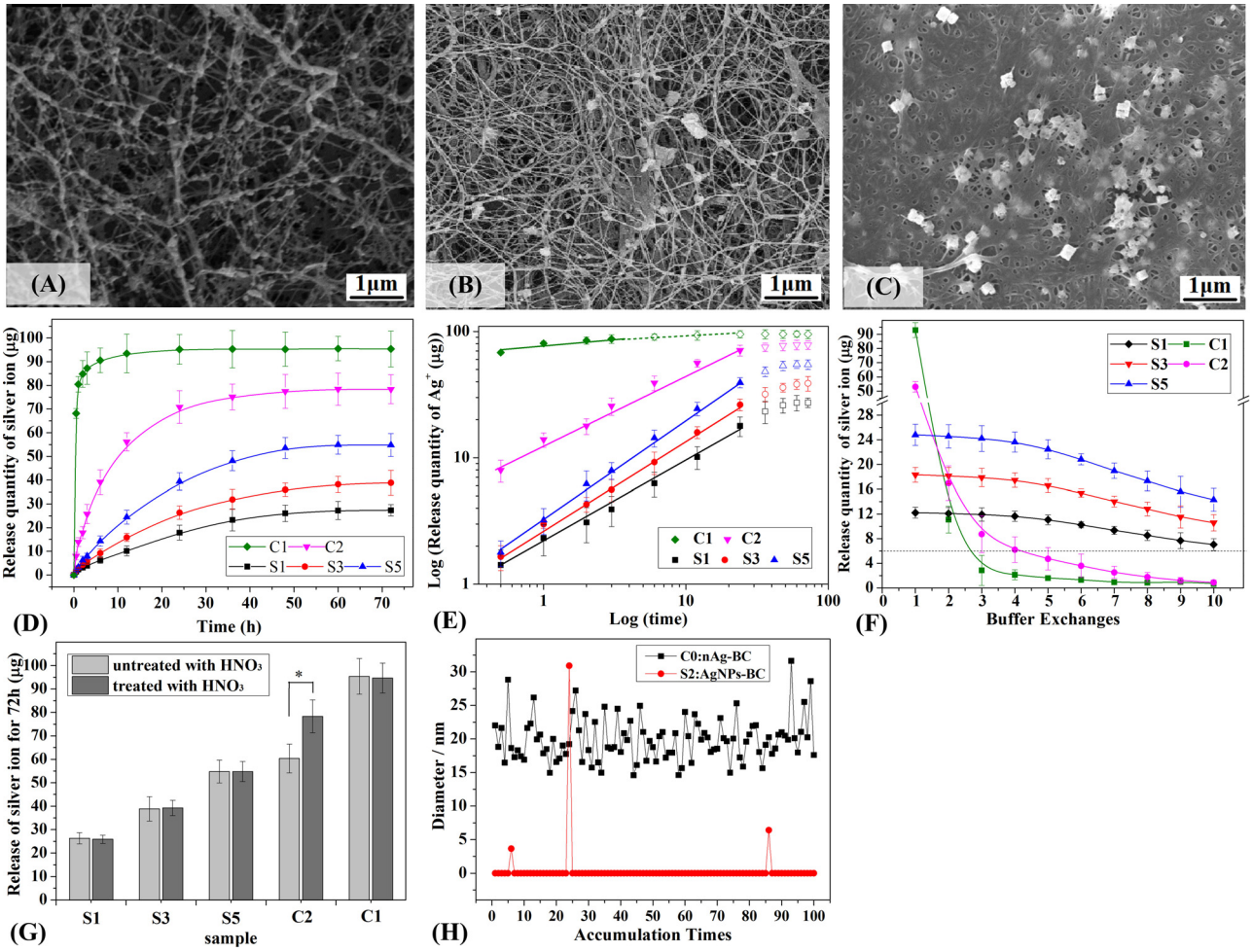


**Fig. 3.** Scanning electron microscopic morphology of (A) AgNP-$BC_{(0.03)}$; (B) nAg-BC; (C) $AgNO_3$-BC. *In vitro* $Ag^+$ releasing properties of AgNP-BC and control samples in PBS buffer solution: (D) release quantity changes of silver ion in PBS buffer solution ($n$ = 6 for the test of Ag contains). (E) log(release quantity of $Ag^+$) *vs* log(times) curve; (F) *in vitro* $Ag^+$ releasing properties of AgNP-BC and control samples in the circulation of PBS buffer solution. (G) Release quantity changes of silver ion in PBS buffer solution for 72 h test before and after treatment of nitric acid. (H) The results of laser particle size distributing test of the releasing solution at 72 h. ($C_1$: $AgNO_3$-BC; $C_2$: nAg-BC; $S_1$: AgNP-$BC_{(0.01)}$; $S_3$: AgNP-$BC_{(0.03)}$; $S_5$: AgNP-$BC_{(0.05)}$).

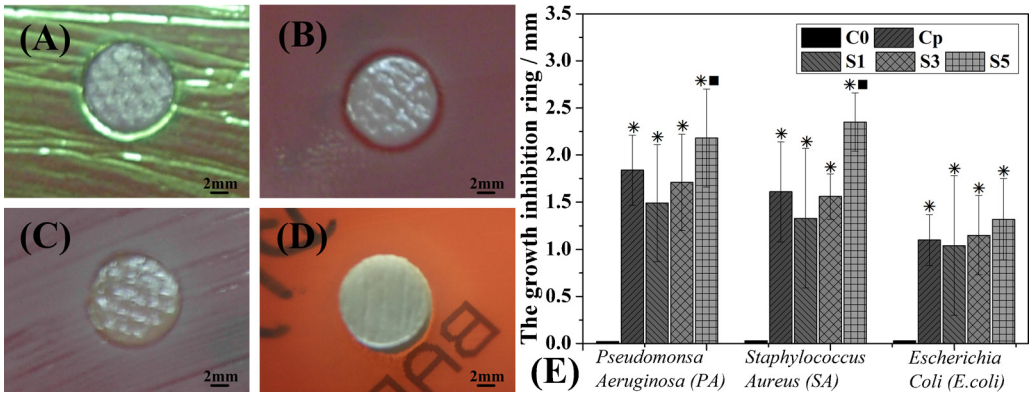


**Fig. 4.** The growth inhibition ring of AgNP-$BC_{(0.03)}$ against (A) *Escherichia coli*, (B) *Staphylococcus aureus*, (C) *Pseudomonas aeruginosa*; (D) the growth inhibition ring of the commercial silver-containing dressing against *Staphylococcus aureus*; (E) datas of the growth inhibition rings of $C_0$, Cp, $S_1$, $S_3$ and $S_5$ against three bacterias. Significance ($p < 0.05$): *, greater than $C_0$; ■, greater than Cp. ($C_0$: BC; Cp: a commercial silver-containing dressing; $S_1$: AgNP-$BC_{(0.01)}$; $S_3$: AgNP-$BC_{(0.03)}$; $S_5$: AgNP-$BC_{(0.05)}$).

from both Ag nanoparticles attached on BC and leached in PBS in coupling with diffusion of Ag nanoparticles, therefore release rate was faster than that of AgNP-BC.

### 3.3. Antimicrobial effects of AgNP-BC

The antibacterial activities of AgNP-BC membranes and a commercial silver-containing dressing as a positive control against *E. coli*, *S. aureus* and *P. aeruginosa*, which are all common bacteria of wound infection, were measured by the disk diffusion method after 24 h incubation at 37 °C (Fig. 4(A)–(C)). It was found that Ag nanoparticles impregnated BC composites developed an inhibition ring zone against all three kinds of bacteria with 1.04–2.35 mm in diameter (Fig. 4(E) – $S_1$, $S_3$, $S_5$). No inhibition zone was observed for the pure BC membrane as control (Fig. 4(E) – $C_0$). This clearly demonstrates that the antimicrobial activity of AgNP-BC is only attributed to the presence of Ag nanoparticles impregnated into BC rather than BC itself. Furthermore, a commercial silver-containing dressing was setted as a positive control (Fig. 4(D)). The growth inhibition rings of the commercial silver-containing dressing was 1.10–1.84 mm (Fig. 4(E) – $C_P$), and it was similar to the inhibition rings of AgNP-BC (no significant difference, $p > 0.05$).

The antibacterial ratios of AgNP-BC membranes against *E. coli*, *S. aureus* and *P. aeruginosa* were tested by the shake flask test method. After 24 h of incubation, there were 98.8–100% reductions of *E. coli*, *S. aureus* and *P. aeruginosa* in all AgNP-BC membranes (Table 3-$S_1$, $S_3$, $S_5$). On the other hand, pure BC provides a biocompatible environment for bacteria's proliferation (Table 3 $C_0$) in which case there were 65.6%, 32.2% and 74.7% increases in the viable counts of *E. coli*, *S. aureus* and *P. aeruginosa*, respectively. The reductions of three bacterias in commercial silver-containing dressing were 99.84%, 100% and 99.58%. Bacteriostatic rate of AgNP-BC membranes and the commercial silver-containing dressing against the three kinds of common bacteria on wound infection were over 99% upon the presence of silver nano-particles, there were no significant difference ($P > 0.05$). The results shown that the antimicrobial effects of AgNP-BC were similar to the antimicrobial effects of the commercial silver-containing dressing (no significant difference, $P > 0.05$). So, AgNP-BC can be use as an antimicrobial wound dressing material.

The results demonstrated that AgNP-BC had good antimicrobial activities against *E. coli* (Gram-negative), *S. aureus* (Gram-positive) and *P. aeruginosa* (Gram-negative). It is also noted that the antibacterial activities against *E. coli and P. aeruginosa were* slightly lower than that against *S. aureus*, which is probably due to the difference in cell walls between Gram-positive and Gram-negative bacteria, this result is similar to the report of Maneerung et al. (2008). The cell wall of the Gram-negative bacteria consist of lipids, proteins and lipopolysaccharides (LPS) which provide effective protection against biocides whereas the Gram-positive bacteria do not consist LPS (Feng, Wu, Chen, Cui, Kim, & Kim, 2000; Maneerung et al., 2008)). In addition, the great affect in Gram-negative bacteria may due to the electrostatic interactions which occur between the cell walls of bacteria and nanoparticle (Neal, 2008). And other factors, such as the form of bacteria species, size and shape of nanoparticles will influence the antibacterial activity of AgNP-BC too (Pal, Tak, & Song, 2007).

**Table 3**
CFU/mL at 0 h and 24 h contact time intervals with the BC membrane containing silver against (A) *Escherichia coli*, (B) *Staphylococcus aureus* and (C) *Pseudomonas aeruginosa*. ($C_0$: BC; Cp: a commercial silver-containing dressing; $S_1$: AgNP-$BC_{(0.01)}$; $S_3$: AgNP-$BC_{(0.03)}$; $S_5$: AgNP-$BC_{(0.05)}$).

| | | $C_0$ | $C_p$ | $S_1$ | $S_3$ | $S_5$ |
|---|---|---|---|---|---|---|
| (A) | 0 h | $1.0 \times 10^5$ | $1.0 \times 10^5$ | $1.0 \times 10^5$ | $1.0 \times 10^5$ | $1.0 \times 10^5$ |
| | 24 h | $1.6 \times 10^5$ | $2.7 \times 10^2$ | $8.2 \times 10^2$ | $1.4 \times 10^2$ | 0 |
| | Reduction | −65.60% | 99.73% | 99.18% | 99.86% | 100% |
| | Bacteriostatic rate | – | 99.84% | 99.50% | 99.92% | 100% |
| (B) | 0 h | $1.0 \times 10^5$ | $1.0 \times 10^5$ | $1.0 \times 10^5$ | $1.0 \times 10^5$ | $1.0 \times 10^5$ |
| | 24 h | $1.3 \times 10^5$ | 0 | 0 | 0 | 0 |
| | Reduction | −32.20% | 100% | 100% | 100% | 100% |
| | Bacteriostatic rate | – | 100% | 100% | 100% | 100% |
| (C) | 0 h | $1.0 \times 10^5$ | $1.0 \times 10^5$ | $1.0 \times 10^5$ | $1.0 \times 10^5$ | $1.0 \times 10^5$ |
| | 24 h | $1.7 \times 10^5$ | $7.4 \times 10^3$ | $1.1 \times 10^3$ | $9.7 \times 10^2$ | $3.8 \times 10^2$ |
| | Reduction | −74.70% | 99.26% | 98.88% | 99.03% | 99.62% |
| | Bacteriostatic rate | – | 99.58% | 99.36% | 99.45% | 99.78% |

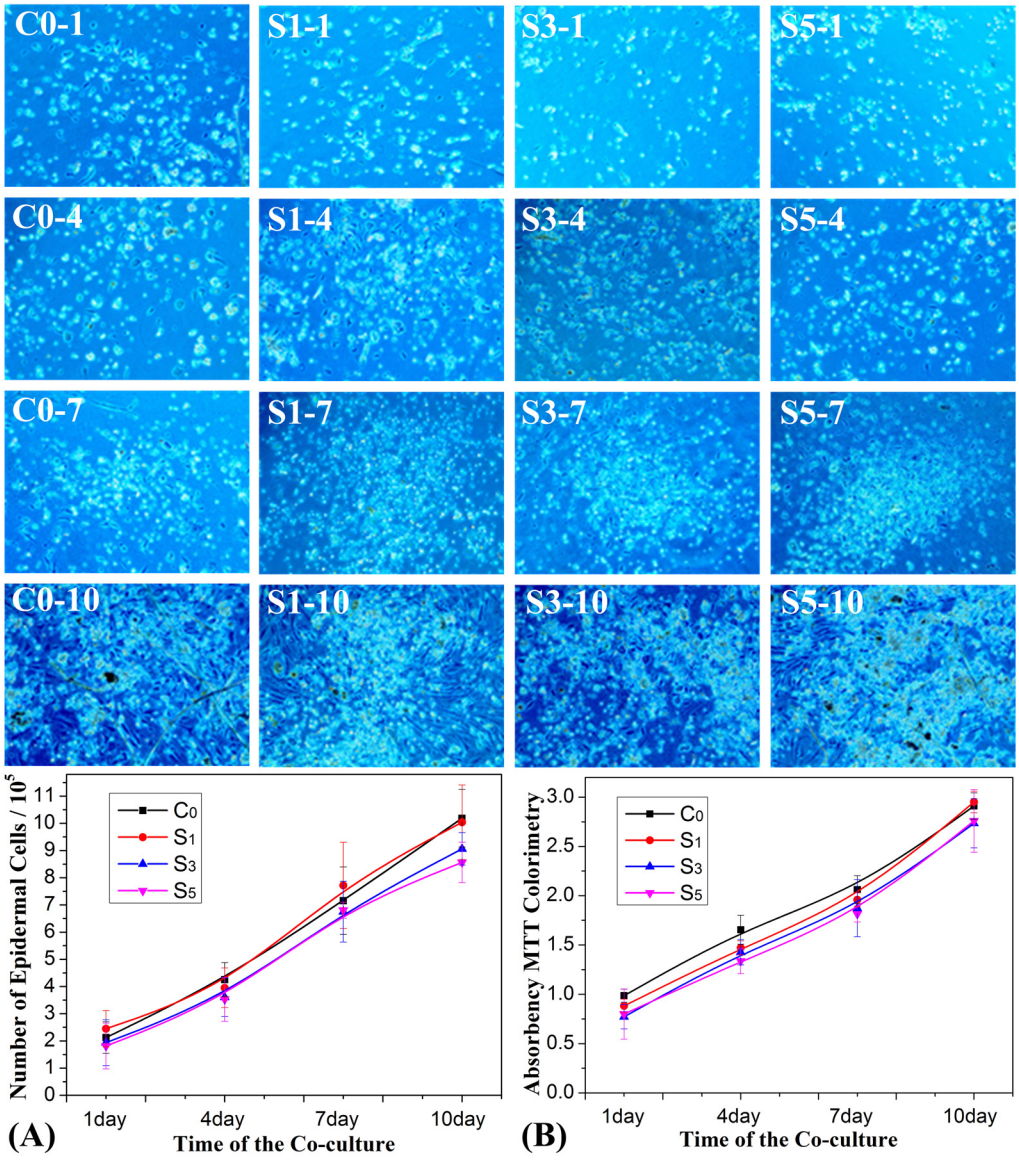


**Fig. 5.** Epidermal cell morphologies of different samples after 1, 4, 7, and 10 days: $C_0$: BC; $S_1$: AgNP-BC$_{(0.01)}$; $S_3$: AgNP-BC$_{(0.03)}$; $S_5$: AgNP-BC$_{(0.05)}$. (A) Epidermal cell numbers after co-cultivating for 1, 4, 7, and 10 days; (B) MTT results of epidermal cells co-cultivated with different samples for 1, 4, 7, and 10 days. Significance ($p < 0.05$): * greater than $C_0$.

### 3.4. Cytotoxicity of AgNP-BC for epidermal cells

The biocompatibility of AgNP-BC was evaluated by co-culturing with epidermal cells of neonatal rats on the 1st, 4th, 7th and 10th day. Cell proliferations and morphologic changes are shown in Fig. 5, where the orbicular transparent small cells observed under optical microscope are epidermal cells.

After culturing for 1 day, epidermal cells were sparsely spereaded more or less everywhere with some noticible dense cell domains. Most epidermal cells appeared in round shape. There were no significant differences between groups. On the 4th day, the number of cells increased obviously with more rounder and larger flat epidermall cells produced, demonstrating that epidermal cell proliferation had begun. Cells continued the growth in well spread ways on the 7th day. In the meantime, epidermal cells started to give rise to fibroblasts in each group with spindle-shaped or irregular triangular morphology. After culturing for 10 days, more fibroblasts grew in all groups and then converged to form large areas in the culture medium. As a result, epidermal cells were gradually masked by the fibroblasts. There were no significant differences among groups.

The observation above showed that there were no significant differences between pure BC ($C_0$) and AgNP-BC ($S_1$, $S_3$ and $S_5$), indicating that AgNP-BC possesed good biocompatibility similar to BC. The favorable environment provided by AgNP-BC encouraged epidermal cells to differentiate into fibroblasts. AgNP-BC showed low toxicity and supported the growth of epidermal cells and fibroblasts. This will be further proven by the following statistic analysis of cellular proliferation and viability of cell growth.

To investigate AgNP-BC's influence on the cellular proliferation, the hemocytometer was used to carry out the test and the results were analyzed in Fig. 5(A). The cell number of all the groups was 80% greater than the control sample (the polystyrene cell culture plate), indicating that the harmful effects of AgNP-BC on cell proliferation were relatively low. Though AgNP-BC inhibited the cell growth to some degree, the number of epidermal cells increased progressively as increasing the culture time with great significance. This statistic measurement further quantifies the growth of epidermal cells

observed in Fig. 5. Hence, the effects of AgNP-BC on cellular proliferation are limited, which will be further investigated using the rat model *in vivo*.

The MTT data describe the relative viability of epidermal cells growing on different samples. The results analyzed in Fig. 5(B) are comparable since the same number of cells was added to all samples. The formazan absorbance indicates that the epidermal cells seeded onto the control sample (the polystyrene cell culture plate) and different membranes were able to convert MTT into a blue formazan product. Though the BC sample exhibited slightly higher MTT absorbance results than the AgNP-BC samples, there were no obvious differences between BC and AgNP-BC. Furthermore, with increasing culture time, the viability of cells on each samples increased significantly. Therefore, it can be concluded that the addition of the AgNPs to BC did not affect the cytocompatibility of the membrane greatly.

The *in vitro* experimental results demonstrated AgNP-BC samples had relatively low cytotoxicity because of the slow releasing of $Ag^+$ and little leakage of Ag nanoparticles, which is an essential characteristic for biomaterials as wound dressing. The positive effects of AgNP-BC on cells *in vitro* encouraged to carry on the following investigation *in vivo*.

## 4. Conclusions

To conclude, *in situ* synthesis and deposition of silver nanoparticles into BC fibrous membrane has been successfully developed through the reaction of Tollens' reagent under ambient conditions. BC nanofibres and their interconnective nanoporous structure played roles of reactive template and confined nanoreactors during the reaction. The resulting uniform spherical silver nano-particles were evenly distributed in the network of BC gel-membranes forming a robust hybrid nanostructure with tailorable Ag loading. Strong adhesion between Ag nanoparticles and BC nano-fibers was proven to prevent any leakage of Ag nanoparticles from BC network, and therefore to minimise the potential toxicity of nanoparticles.

AgNP-BC hybrid nanostructure offered excellent and sustainable controllability of $Ag^+$ release, following an exponential power law, with exponent $n$ dependent of Ag content. Silver ion release from AgNP-BC is slow in PBS solution with only 16.5% of $Ag^+$ released in 72 h, in contrast to two control groups with 78.35% and 95.39%. Regardless the slow $Ag^+$ release, AgNP-BC still exhibited significant antibacterial rates with more than 99% reduction against *E. coli*, *S. aureus* as well as *P. aeruginosa*, and the antimicrobial effects of AgNP-BC were similar to a commercial silver-containing dressing. In addition, AgNP-BC allows attachment and growth of epidermal cells without cytotoxicity emerging in co-culture with epidermal cells. In short, systematic *in vitro* results manifest that nanostructural AgNP-BC gel-membrane is promising for antimicrobial wound dressing with good biocompatibility to promote scald wound healing.

## Acknowledgements

This study is financially supported by National Natural Science Foundation of China Project (Grant Nos. 51073024 and 51273021), and the National Science and Technology Support Project of China (Grant No. 2011BAK15B04).

## References

Ahamed, M., Karns, M., Goodson, M., Rowe, J., Hussain, S. M., Schlager, J. J., et al. (2008). DNA damage response to different surface chemistry of silver nanoparticles in mammalian cells. *Toxicology and Applied Pharmacology*, *233*(3), 404–410.

Andersson, J., Stenhamre, H., Backdahl, H., & Gatenholm, P. (2010). Behavior of human chondrocytes in engineered porous bacterial cellulose scaffolds. *Journal of Biomedical Materials Research Part A*, *94*(4), 1124–1132.

Barud, H. S., Regiani, T., Marques, R. F. C., Lustri, W. R., Messaddeq, Y., & Ribeiro, S. J. L. (2011). Antimicrobial bacterial cellulose-silver nanoparticles composite membranes. *Journal of Nanomaterials*, *2011*, 1–8.

Bodin, A., Bharadwaj, S., Wu, S. F., Gatenholm, P., Atala, A., & Zhang, Y. Y. (2010). Tissue-engineered conduit using urine-derived stem cells seeded bacterial cellulose polymer in urinary reconstruction and diversion. *Biomaterials*, *31*(34), 8889–8901.

Boonme, P., Amnuaikit, Chusuit, & Raknam. (2011). Effects of a cellulose mask synthesized by a bacterium on facial skin characteristics and user satisfaction. *Medical Devices: Evidence and Research*, 77–81.

Brackmann, C., Zaborowska, M., Sundberg, J., Gatenholm, P., & Enejder, A. (2012). In situ imaging of collagen synthesis by osteoprogenitor cells in microporous bacterial cellulose scaffolds. *Tissue Engineering Part C: Methods*, *18*(3), 227–234.

Brown, A. J. (1886). XIX – The chemical action of pure cultivations of bacterium aceti. *Journal of the Chemical Society, Transactions*, *49*, 172–187.

Cai, J., Kimura, S., Wada, M., & Kuga, S. (2009). Nanoporous cellulose as metal nanoparticles support. *Biomacromolecules*, *10*(1), 87–94.

Cai, Z. J., Hou, C. W., & Yang, G. (2012). Preparation and characterization of a bacterial cellulose/chitosan composite for potential biomedical application. *Journal of Applied Polymer Science*, *126*(6), 1488–1494.

Cheng, K.-C., Catchmark, J. M., & Demirci, A. (2011). Effects of CMC addition on bacterial cellulose production in a biofilm reactor and its paper sheets analysis. *Biomacromolecules*, *12*(3), 730–736.

Ciechanska, D., Struszczyk, H., Kazimierczak, J., Guzinska, K., Pawlak, M., Kozlowska, E., et al. (2002). New electro-acoustic transducers based on modified bacterial cellulose. *Fibres & Textiles in Eastern Europe*, *10*(1), 27–30.

Cohen, S. Y., Quentel, G., Egasse, D., Cadot, M., Ingster-moati, I., & Coscas, G. J. (1993). The dark choroid in systemic argyrosis. *Retina*, *13*(4), 312–316.

Czaja, W., Krystynowicz, A., Bielecki, S., & Brown, R. M., Jr. (2006). Microbial cellulose – The natural power to heal wounds. *Biomaterials*, *27*(2), 145–151.

Damm, C., Munsted, H., & Rosch, A. (2007). Long-term antimicrobial polyamide 6/silver-nanocomposites. *Journal of Materials Science*, *42*(15), 6067–6073.

de Santa Maria, L. C., Santos, A. L. C., Oliveira, P. C., Barud, H. S., Messaddeq, Y., & Ribeiro, S. J. L. (2009). Synthesis and characterization of silver nanoparticles impregnated into bacterial cellulose. *Materials Letters*, *63*(9/10), 797–799.

Feng, Q., Wu, J., Chen, G., Cui, F., Kim, T., & Kim, J. (2000). A mechanistic study of the antibacterial effect of silver ions on *Escherichia coli* and *Staphylococcus aureus*. *Journal of Biomedical Materials Research*, *52*(4), 662–668.

Ghule, K., Ghule, A. V., Chen, B. J., & Ling, Y. C. (2006). Preparation and characterization of ZnO nanoparticles coated paper and its antibacterial activity study. *Green Chemistry*, *8*(12), 1034–1041.

Hu, W., Chen, S., Liu, L., Ding, B., & Wang, H. (2011). Formaldehyde sensors based on nanofibrous polyethyleneimine/bacterial cellulose membranes coated quartz crystal microbalance. *Sensors and Actuators B: Chemical*, *157*(2), 554–559.

Hussain, S. M., Braydich-Stolle, L. K., Schrand, A. M., Murdock, R. C., Yu, K. O., Mattie, D. M., et al. (2009). Toxicity evaluation for safe use of nanomaterials: Recent achievements and technical challenges. *Advanced Materials*, *21*(16), 1549–1559.

Ifuku, S., Tsuji, M., Morimoto, M., Saimoto, H., & Yano, H. (2009). Synthesis of silver nanoparticles templated by TEMPO-mediated oxidized bacterial cellulose nanofibers. *Biomacromolecules*, *10*(9), 2714–2717.

Isogai, A., Usuda, M., Kato, T., Uryu, T., & Atalla, R. H. (1989). Solid-state CP/MAS carbon-13 NMR study of cellulose polymorphs. *Macromolecules*, *22*(7), 3168–3172.

Jung, R., Kim, H.-S., Kim, Y., Kwon, S.-M., Lee, H. S., & Jin, H.-J. (2008). Electrically conductive transparent papers using multiwalled carbon nanotubes. *Journal of Polymer Science Part B: Polymer Physics*, *46*(12), 1235–1242.

Jung, R., Kim, Y., Kim, H. S., & Jin, H. J. (2009). Antimicrobial properties of hydrated cellulose membranes with silver nanoparticles. *Journal of Biomaterials Science, Polymer Edition*, *20*(3), 311–324.

Klasen, H. J. (2000). Historical review of the use of silver in the treatment of burns. I. Early uses. *Burns*, *26*(2), 117–130.

Klemm, D., Schumann, D., Udhardt, U., & Marsch, S. (2001). Bacterial synthesized cellulose – Artificial blood vessels for microsurgery. *Progress in Polymer Science*, *26*(9), 1561–1603.

Kumar, A., Vemula, P. K., Ajayan, P. M., & John, G. (2008). Silver-nanoparticle-embedded antimicrobial paints based on vegetable oil. *Nature Materials*, *7*(3), 236–241.

Maneerung, T., Tokura, S., & Rujiravanit, R. (2008). Impregnation of silver nanoparticles into bacterial cellulose for antimicrobial wound dressing. *Carbohydrate Polymers*, *72*(1), 43–51.

Maynard, A. D., Aitken, R. J., Butz, T., Colvin, V., Donaldson, K., Oberdorster, G., et al. (2006). Safe handling of nanotechnology. *Nature*, *444*(7117), 267–269.

Muangman, P., Opasanon, S., Suwanchot, S., & Thangthed, O. (2011). Efficiency of microbial cellulose dressing in partial-thickness burn wounds. *The Journal of the American College of Certified Wound Specialists*, *3*(1), 16–19.

Neal, A. L. (2008). What can be inferred from bacterium–nanoparticle interactions about the potential consequences of environmental exposure to nanoparticles? *Ecotoxicology*, *17*(5), 362–371.

Pal, S., Tak, Y. K., & Song, J. M. (2007). Does the antibacterial activity of silver nanoparticles depend on the shape of the nanoparticle? A study of the gram-negative bacterium *Escherichia coli*. *Applied and Environmental Microbiology*, *73*(6), 1712–1720.

Panyala, N. R., Pena-Mendez, E. M., & Havel, J. (2008). Silver or silver nanoparticles: A hazardous threat to the environment and human health. *Journal of Applied Biomedicine*, *6*(3), 117–129.

Paul, D. R. (2011). Elaborations on the Higuchi model for drug delivery. *International Journal of Pharmaceutics*, *418*(1), 13–17.
Pinto, R. J. B., Marques, P. A. A. P., Neto, C. P., Trindade, T., Daina, S., & Sadocco, P. (2009). Antibacterial activity of nanocomposites of silver and bacterial or vegetable cellulosic fibers. *Acta Biomaterialia*, *5*(6), 2279–2289.
Retegi, A., Algar, I., Martin, L., Altuna, F., Stefani, P., Zuluaga, R., et al. (2012). Sustainable optically transparent composites based on epoxidized soy-bean oil (ESO) matrix and high contents of bacterial cellulose (BC). *Cellulose*, *19*(1), 103–109.
Robson, M. C. (1997). Wound infection: A failure of wound healing caused by an imbalance of bacteria. *Surgical Clinics of North America*, *77*(3), 637–650.
Rosenman, K., Moss, A., & Kon, S. (1979). Argyria: Clinical implications of exposure of silver nitrate and silver oxide. *Journal of Occupational Medicine*, *21*(6), 430–435.
Ruparelia, J. P., Chatterjee, A. K., Duttagupta, S. P., & Mukherji, S. (2008). Strain specificity in antimicrobial activity of silver and copper nanoparticles. *Acta Biomaterialia*, *4*(3), 707–716.
Shah, J., & Brown, R. M., Jr. (2005). Towards electronic paper displays made from microbial cellulose. *Applied Microbiology and Biotechnology*, *66*(4), 352–355.
Shezad, O., Khan, S., Khan, T., & Park, J. K. (2010). Physicochemical and mechanical characterization of bacterial cellulose produced with an excellent productivity in static conditions using a simple fed-batch cultivation strategy. *Carbohydrate Polymers*, *82*(1), 173–180.
Shi, Q., Li, Y., Sun, J., Zhang, H., Chen, L., Chen, B., et al. (2012). The osteogenesis of bacterial cellulose scaffold loaded with bone morphogenetic protein-2. *Biomaterials*, *33*(28), 6644–6649.
Siepmann, J., & Peppas, N. A. (2011). Higuchi equation: Derivation, applications, use and misuse. *International Journal of Pharmaceutics*, *418*(1), 6–12.
Solway, D. R. (2010). Microbial cellulose wound dressing in the treatment of skin tears in the frail elderly. *Wounds – A Compendium of Clinical Research and Practice*, *22*(1), 17–19.
Sureshkumar, M., Siswanto, D. Y., & Lee, C.-K. (2010). Magnetic antimicrobial nanocomposite based on bacterial cellulose and silver nanoparticles. *Journal of Materials Chemistry*, *20*(33), 6948–6955.
Ul-Islam, M., Ha, J. H., Khan, T., & Park, J. K. (2013). Effects of glucuronic acid oligomers on the production, structure and properties of bacterial cellulose. *Carbohydrate Polymers*, *92*(1), 360–366.
Wei, B., Yang, G., & Hong, F. (2011). Preparation and evaluation of a kind of bacterial cellulose dry films with antibacterial properties. *Carbohydrate Polymers*, *84*(1), 533–538.
Wijnhoven, S. W., Peijnenburg, W. J., Herberts, C. A., Hagens, W. I., Oomen, A. G., Heugens, E. H., et al. (2009). Nano-silver – A review of available data and knowledge gaps in human and environmental risk assessment. *Nanotoxicology*, *3*(2), 109–138.
Yan, Z., Chen, S., Wang, H., Wang, B., & Jiang, J. (2008). Biosynthesis of bacterial cellulose/multi-walled carbon nanotubes in agitated culture. *Carbohydrate Polymers*, *74*(3), 659–665.
Yang, G., Xie, J., Hong, F., Cao, Z., & Yang, X. (2012). Antimicrobial activity of silver nanoparticle impregnated bacterial cellulose membrane: Effect of fermentation carbon sources of bacterial cellulose. *Carbohydrate Polymers*, *87*(1), 839–845.
Yang, Y., Jia, J., Xing, J., Chen, J., & Lu, S. (2013). Isolation and characteristics analysis of a novel high bacterial cellulose producing strain *Gluconacetobacter intermedius* CIs26. *Carbohydrate Polymers*, *92*(2), 2012–2017.
Yoshino, K., Matsuoka, R., Nogami, K., Yamanaka, S., Watanabe, K., Takahashi, M., et al. (1990). Graphite film prepared by pyrolysis of bacterial cellulose. *Journal of Applied Physics*, *68*(4), 1720–1725.
Zaborowska, M., Bodin, A., Backdahl, H., Popp, J., Goldstein, A., & Gatenholm, P. (2010). Microporous bacterial cellulose as a potential scaffold for bone regeneration. *Acta Biomaterialia*, *6*(7), 2540–2547.
Zhang, Y., Peng, H., Huang, W., Zhou, Y., & Yan, D. (2008). Facile preparation and characterization of highly antimicrobial colloid Ag or Au nanoparticles. *Journal of Colloid and Interface Science*, *325*(2), 371–376.